Fire effects on net radiation and energy partitioning: Contrasting responses of tundra and boreal forest ecosystems

S. D. Chambers,[1] J. Beringer,[2] J. T. Randerson,[3] and F. S. Chapin III[4]

Received 29 July 2004; revised 16 January 2005; accepted 16 February 2005; published 5 May 2005.

[1] The net radiation available to drive surface-atmosphere exchange is strongly influenced by albedo and surface temperature. Tower-based microclimatic and eddy covariance measurements in typical Alaskan black spruce and tundra ecosystems before and immediately after fire indicated a 10% decrease in net radiation over the burned spruce stand but a 12% increase in net radiation over the burned tundra surface. In both cases, there was increased partitioning of net radiation into sensible heat flux. In terms of absolute fluxes, however, fire increased average sensible heating over tundra by ~50 W m^{-2} but caused little change in average sensible heat flux over the black spruce forest. This difference in fire effects occurred because fire altered the canopy characteristics (including surface roughness) more strongly in the forest than in the tundra, leading to a greater reduction in surface-atmosphere coupling over the forest.

Citation: Chambers, S. D., J. Beringer, J. T. Randerson, and F. S. Chapin III (2005), Fire effects on net radiation and energy partitioning: Contrasting responses of tundra and boreal forest ecosystems, *J. Geophys. Res.*, *110*, D09106, doi:10.1029/2004JD005299.

1. Introduction

[2] Fire plays an important role in the functioning and spatial heterogeneity of boreal forests. Under current climatic conditions, ~3 million hectares of North American boreal forest burn annually [*Kasischke et al.*, 1995]. This rate has doubled in western North America in the last 40 years and has been linked to high-latitude warming [*Murphy et al.*, 2000]. The boreal forest is the second most extensive biome on Earth, occupying 17% of the ice-free terrestrial surface [*Whittaker*, 1975]. If changes in fire regime (frequency, size, and severity) induce changes in energy exchange between the land and the atmosphere, this could have important climatic consequences [*Bonan et al.*, 1992; *Thomas and Rowntree*, 1992; *Chapin et al.*, 2000a]. However, few quantitative measurements are available on the micrometeorological effects of fire [*Amiro*, 2001; *Amiro et al.*, 1999, 2003; *Chambers and Chapin*, 2002; *Röser et al.*, 2002]. Early measurements by *Rouse* [1976] examined the radiation balance but neglected the surface energy budget. Although a more comprehensive suite of airborne measurements were made over some Canadian boreal forest stands in early postfire succession by *Amiro et al.* [1999], they are limited in temporal resolution. More recently, *Amiro* [2001] reported a brief paired tower comparison between a 1 year old burned and mature jack pine/black spruce stand. The aim of this study was to characterize net radiation and its relative partitioning into turbulent fluxes between black spruce and tundra, two common high-latitude ecosystem types with vastly different surface characteristics, before and immediately after fire. We made tower-based microclimatic and eddy covariance flux measurements over typical burned and unburned black spruce forests and lichen-dominated tundra for short periods during the 1999 growing season. Our findings contradict the conventional wisdom that the decrease in albedo after fire would substantially increase the sensible heat flux to the atmosphere immediately after disturbance regardless of the prefire canopy characteristics.

2. Methods

2.1. Theory

[3] The supply of radiative energy to the Earth and its redistribution maintain a thermal equilibrium at the surface through a combination of the radiation balance and surface energy budget:

$$Q^* = (K_\downarrow - K_\uparrow) + (L_\downarrow - L_\uparrow) = H + \mathrm{LE} + G + \Delta S, \quad (1)$$

where $K_\downarrow$ and $K_\uparrow$ are the components of incoming and reflected shortwave radiation (W m^{-2}); $L_\downarrow$ and $L_\uparrow$ are the components of incoming and emitted longwave radiation (W m^{-2}); Q^* is the net radiation (the excess energy remaining at the surface-atmosphere interface, W m^{-2}); H, LE, and G are the sensible, latent, and ground heat fluxes (W m^{-2}) that redistribute the bulk of the net radiation; and ΔS is the energy storage that represents a combination of

[1]Environment Division, Australian Nuclear Science and Technology Organization, Menai, New South Wales, Australia.
[2]School of Geography and Environmental Science, Monash University, Clayton, Victoria, Australia.
[3]Department of Earth System Science, University of California, Irvine, California, USA.
[4]Institute of Arctic Biology, University of Alaska Fairbanks, Fairbanks, Alaska, USA.

0148-0227/05/2004JD005299$09.00

Table 1. Summary of Site Locations, Campaign Dates, Typical Midday Insolation ($K_\downarrow$), and Key Site Characteristics

Site	Unburned Spruce	Burned Spruce	Unburned Tundra	Burned Tundra
Name and location	Hajdukovich Creek (63°48′N, 145°06′W)	Donnelly Flats (63°54′N, 145°44′W)	Seward Peninsula (64°50.5′N, 163°41.6′W)	Seward Peninsula (65°12.15′N, 164°18.48′W)
Observation period (1999)	16 July to 1 August	3 July to 1 August	28 July to 3 August	28 July to 3 August
Incoming shortwave, W m^{-2}	754	754	615	615
Radiation efficiency, $Q^*/K_\downarrow$	0.76 ± 0.004	0.68 ± 0.003	0.68 ± 0.027	0.76 ± 0.002
Albedo, α	0.09 ± 0.0004	0.07 ± 0.0005	0.19 ± 0.001	0.05 ± 0.002
Roughness length, z_o, m	0.70	0.09	0.04	0.01
Normalized heat flux, $H/K_\downarrow$	0.40	0.43	0.20	0.27

energy sinks, including heat storage within the canopy biomass, heat and water vapor storage within the canopy airspace, and the energy consumed by photosynthesis [*Oke*, 1987]. Total energy storage typically accounts for less than 10% of the net radiation on an hourly basis [*McCaughey and Saxon*, 1998; *Meesters and Vugts*, 1996] and is generally negligible compared to the measurement accuracy of the primary redistribution processes.

[4] Since incoming shortwave radiation and column average sky temperature are relatively constant over short timescales near noon under clear-sky conditions, it follows from the radiation balance (equation (2)) that under these conditions, albedo and surface temperature have the greatest influence on net radiation [*Betts and Ball*, 1997]:

$$Q^* = (1-\alpha)K_\downarrow + \sigma\left(\varepsilon_{\mathrm{sky}}T_{\mathrm{sky}}^4 - \varepsilon_{\mathrm{surf}}T_{\mathrm{surf}}^4\right). \qquad (2)$$

Here α is the surface albedo, σ is the Stefan-Boltzman constant (5.67×10^{-8} W m^{-2} K^{-4}), T is absolute temperature (K), and ε is the emissivity.

[5] Net radiation is determined by stand properties, insolation, and moisture availability. Since it is the intention of this study to focus on the influence of stand characteristics on net radiation specifically, we have (1) normalized net radiation for each stand by its respective value of incoming shortwave radiation ($Q^*/K_\downarrow$) to account for changes in incoming shortwave radiation between sites, (2) restricted our period of interest to 2 hours either side of local solar noon when fluxes are largest and there are no rapid changes in the components of the surface energy budget, and (3) selected periods of similar climatic conditions (clear-sky conditions and not immediately following rain) for the black spruce and tundra site pairs. The ratio $Q^*/K_\downarrow$ is hereinafter referred to as the "radiation efficiency" (i.e., net radiation per unit of incoming shortwave radiation) [e.g., *Baldocchi et al.*, 2000].

[6] The magnitude of the net longwave radiation ($L^* = L_\downarrow - L_\uparrow$) contribution to the radiation balance depends on how efficient a given canopy is at shedding energy to the atmosphere (the surface-atmosphere coupling), which, in turn, is related to canopy architecture [*Jarvis and McNaughton*, 1986]. Some key canopy attributes that influence the efficiency of energy transfer to the near-surface atmosphere are the relative surface area, density, and shape of the canopy elements. Consequently, if fire significantly affects the canopy architecture, it could alter the efficiency of energy transfer to the atmosphere. Two trademarks of spruce canopies are a low albedo and high surface roughness. The low albedo results from efficient radiation trapping [*Stenberg et al.*, 1995] and dark canopy elements [*Jarvis et al.*, 1976], and the high roughness is largely attributable to the irregular crown heights and tapered shape of the coniferous crowns [*Baldocchi et al.*, 2000]. The crown shape plays at least two key roles in surface atmosphere exchange: (1) It enables turbulent mixing throughout the entire depth of the canopy, particularly in stands of low to moderate stem density, providing a highly efficient surface-atmosphere coupling for the exchange of heat and various scalars [*Oke*, 1987], and (2) it enables deep penetration of insolation throughout the canopy and the understory [*Baldocchi et al.*, 1997], such that the energy is distributed over a large surface area.

2.2. Measurements

[7] Tower-based microclimatic and eddy covariance measurements were used to characterize the radiation balance and energy budget above unburned and recently burned black spruce and tundra ecosystems in central and western Alaska, respectively (Table 1) [*Chambers and Chapin*, 2002; J. Beringer et al., Partitioning of surface energy exchanges along a tundra-forest vegetation transition: The importance of canopy structure, submitted to *Agricultural and Forest Meteorology*, 2005]. Both fires occurred early in the summer of 1999, and in both cases, measurements were made in July, less than a month after the fires. Although instrument heights differed according to the canopy heights, identical instrumentation was used for the measurements at each site. We used 15 m towers over the spruce forest stands and 10 m towers over the tundra sites. Primary radiation measurements were made as close as practical to the top of the towers (10–14 m) to minimize the potential of shading and to maximize the surface area within the effective sensor footprint [*Schmid*, 1997]. At the spruce sites, measurements of net radiation and incoming shortwave radiation were also made at ~0.20 of the mean canopy height (~0.50 m), which was above the understory vegetation of the unburned stand. Eddy covariance measurements were made at 4–5 m above the average canopy height (or ground) over the burned and unburned spruce forest stands and at 2–3 m above the surface in the tundra sites. Budget closure errors were slightly larger over the burned stands. Overall, discrepancies were less than $0.2Q^*$ during times of positive net radiation (neglecting storage terms), indicating that advective effects were small and the measurement technique was satisfactory.

[8] A combination of a three-dimensional ultrasonic anemometer (Gill Solent, horizontally symmetric) and a closed-path infrared gas analyser (LI-COR Inc., model 6262) were used to estimate the fluxes of sensible and latent heat via the eddy covariance method [*Baldocchi et al.*, 1988]. A 3 mm internal diameter "Bev-A-Line" intake

tube was used for the gas analyzer with an aspiration rate of ~7 L min^{-1} that ensured turbulent flow in the sample line, and 1.5 m of externally insulated copper tubing was placed inline to minimize temperature-induced density fluctuations [*Leuning and Judd*, 1996]. The observations were logged at 10 Hz with a laptop computer.

[9] Climate sensors were scanned every 20 s, and 10 min averages were recorded on a data logger (Campbell Scientific Inc., CR10). Incoming and reflected shortwave as well as incoming and emitted longwave radiation were measured using pairs of pyranometers (Eppley Inc., model PSP) and pyrgeometers (Eppley Inc., model PIR), respectively. An independent estimate of net radiation above each surface was made using a Frischen-type net radiometer (Radiation and Energy Balance Systems (REBS), model Q7.1) with a wind speed–dependant dome-cooling correction applied to the results [*Radiation and Energy Balance Systems*, 1994]. Profiles of air temperature and water vapor content beneath the level of the sonic anemometer were measured using temperature/relative humidity probes (Vaisala, model HMP45C). A separate portable infrared sensor (Everest Interscience Inc., 4000ALCS) was also available for spot surface temperature estimates. Wind speed at the radiometer height, as well as near the canopy/surface, was measured using cup anemometers (R. M. Young, 03101). Ground heat flux was estimated via the combination method [*Oke*, 1987] using heat flux plates (REBS, HFT3) and integrated soil temperature measurements in the soil layer above the heat flux plate (REBS, PRT) at four representative locations. Ground heat flux for each tower site was estimated using the area-weighted average of ground heat fluxes measured in each of the representative microsite types (e.g., lichen-dominated versus moss-dominated microsites). The 10 min climate data were aggregated to 30 min blocks to match the eddy covariance data. Unless otherwise stated, values reported represent an average of the available 30 min data for 2 hours on either side of local solar noon. Depending on the measurement site, observation periods varied in duration from approximately 1 to 3 weeks (Table 1).

[10] A vegetation survey was conducted within the measurement footprint of each tower. These surveys indicated that the burned forest and tundra sites both had a canopy architecture (vegetation height and density) that was similar to their respective unburned control sites before fire.

[11] The mean height of trees greater than 1 m in the unburned black spruce (*Picea mariana*) stand was 2.7 m. As an indication of the unevenness of the canopy height, the maximum and 90th percentile heights were 7.9 and 4.9 m, respectively. The stem density of trees greater than 1 m was 13,800 ha^{-1} with a mean diameter at breast height (DBH) of ~6 cm. The predominant ground cover was feathermoss and foliose lichens. The cover of herbaceous and woody understory species averaged 60%. At the burned spruce site, resprouting growth composed less than 1% of the total ground cover. The fire was severe, so all but the most substantial of the above ground biomass was consumed, leaving only the trunks of large trees and parts of thick branches. The mean height of the standing dead trees greater than 1 m remaining after fire was 3.9 m, with a stem density of only 4500 ha^{-1}. Typically, 2–5 cm of ash and charred organic material remained above the mineral soil horizon. Patches of exposed mineral soil were evident, as well as patches of windblown loess that had accumulated within the moss/lichen layer and had been exposed by the fire. Overall, ~80% of the surface within the measurement footprint was charred black, and the rest was a sandy color.

[12] The canopy of the unburned tundra site was typically 15–30 cm tall and consisted mainly of sedges (16%) and dwarf shrubs (13%). The dominant tundra ground cover species were fruticose lichens (31%) and *Sphagnum* moss (24%). The tundra burn was of moderate severity. Most of the lichen, green moss, and aboveground vascular vegetation were consumed, leaving a blackened organic surface. Hot, dry weather conditions at that site in June had desiccated the uppermost 10–15 cm of vegetation and organic matter, but the subsurface material was still frozen and saturated. As a result the burning was not very deep. At the time of measurements the only live vegetation present was resprouting leaves of the sedge *Eriophorum vaginatum* (3% cover) and small patches of unburned *Sphagnum* moss. Microscale variation in soil moisture status, chiefly a result of the distribution of *Sphagnum* moss and tussocks of *Eriophorum vaginatum*, resulted in a more heterogeneous burn than in the black spruce stand.

[13] Roughness length (z_o) over each surface was estimated in the following manner:

$$z_o = \frac{(z-d)}{\exp\left(\frac{Uk}{u^*}\right)}, \tag{3}$$

where z is the measurement height (m), d is the displacement height (m), U is the mean wind speed at sonic height (m s^{-1}), k is the Von Karman constant (0.4), and u^* is the friction velocity (m s^{-1}). Data were selected that most closely represented neutral stability ($-0.2 < z/L < 0.2$, where L is the Obukhov length), when the mean wind speed was greater than 1 m s^{-1}. All times reported in this paper are local Alaskan time, and unless otherwise stated, the variability quoted about mean values is the standard error.

3. Results

3.1. Radiation Budget

[14] Under clear-sky conditions, fire reduced the near-noon radiation efficiency ($Q^*/K_\downarrow$) of the spruce forest by ~10% (from 0.76 to 0.68) but increased the radiation efficiency of the tundra by ~12% (from 0.68 to 0.76) (Table 1). To put these results in context with mean conditions experienced over the whole measurement period and the remainder of the diurnal cycle, Figure 1 provides a diurnal composite plot of the mean radiation components for each site. Here the 30 min mean values have been grouped into hourly bins, and the 90th percentile values have been included as the best unbiased estimate of clear-sky conditions based on the complete data set for each site. The near-noon window has been indicated for reference purposes.

[15] When all measurement conditions were taken into account (Figure 1), it was found that while the presence of cloud and a moister surface had little effect on the radiation efficiency of the unburned spruce stand, there was less of a reduction in radiation efficiency for the burned spruce stand,

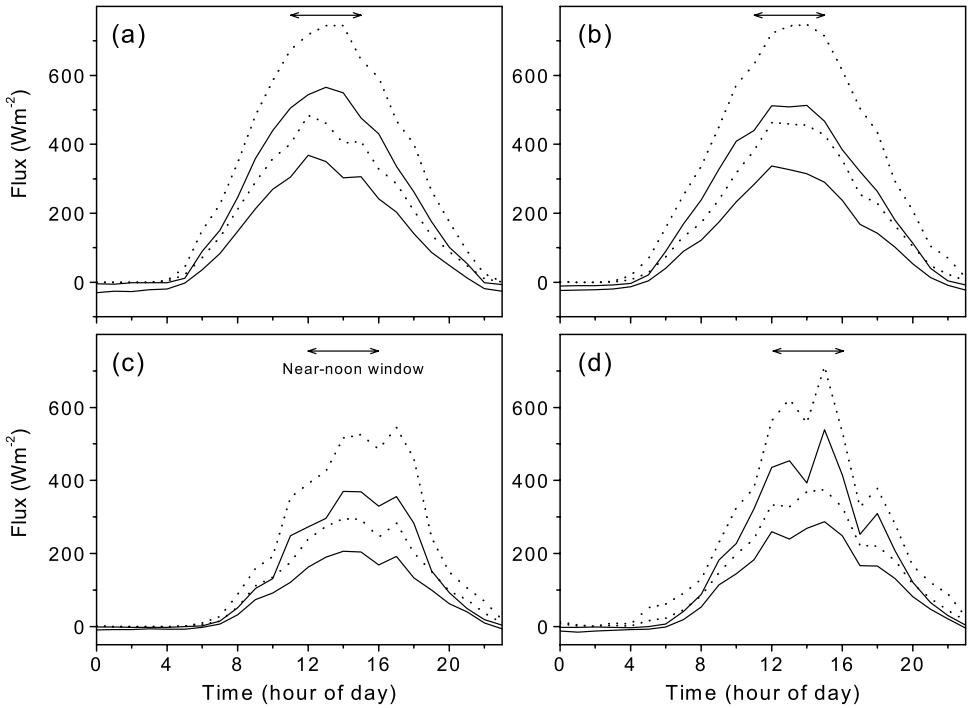

Figure 1. Diurnal composite plots of incoming shortwave (dotted lines) and net (solid lines) radiation over the respective measurement periods for the (a) spruce control, (b) burned spruce, (c) tundra control, and (d) burned tundra sites. Bottom lines represent mean values. Top lines represent the 90th percentile values, which closely resemble clear-sky conditions. Note the difference in site locations as detailed in Table 1.

from ~0.76 to ~0.71 (6.6%). Likewise, under mean conditions, there was a smaller increase in radiation efficiency over tundra as a result of fire, from 0.70 to 0.74 (~6%). The similarities in response to fire observed between mean and clear-sky conditions indicate that the changes in radiation efficiency of each stand were primarily caused by fire-induced changes in albedo and surface temperature rather than atmospheric conditions.

[16] The mean diurnal minimum albedo of the unburned spruce forest (0.09) was less than half that of the unburned tundra (0.19) (Table 1). The diurnal amplitude of the albedo fluctuation over the tundra site was slightly larger than over the forest (Figure 2), indicative of a smoother surface that intercepted and trapped less incident radiation at low solar angles. In spite of the large difference in albedo between the spruce forest and tundra sites prior to burning, the values of postfire albedo for the spruce forest and tundra sites were not substantially different. Although fire reduced the mean diurnal minimum albedo of the spruce forest by only 24% (to 0.07), the corresponding decrease in albedo for the tundra site was 75% (to 0.05). These reductions of albedo correspond to an ~3% and ~20% increase in net radiation for the spruce and tundra sites, respectively, based on typical midday growing season values (Table 1).

[17] Canopy temperature determines the longwave radiation emitted by an ecosystem. On a clear-sky day the average near-noon canopy temperature of the unburned spruce forest was 26.7 ± 0.21°C. This was calculated using emitted longwave radiation and an emissivity of 0.98 (estimated independently, data not shown). This emissivity

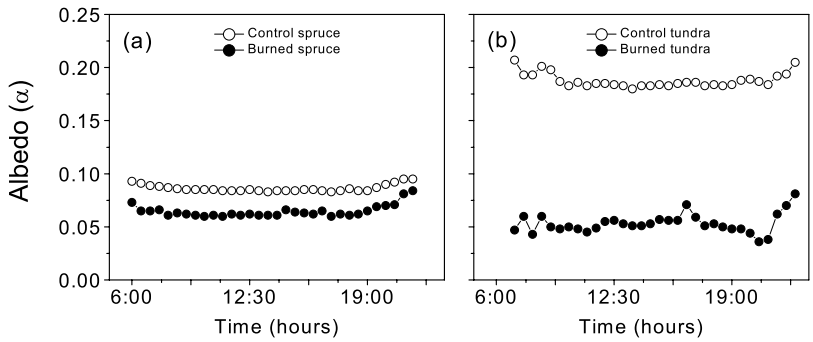

Figure 2. Diurnal course of albedo over the (a) spruce forest and (b) tundra sites. Open and solid circles denote prefire and postfire values, respectively.

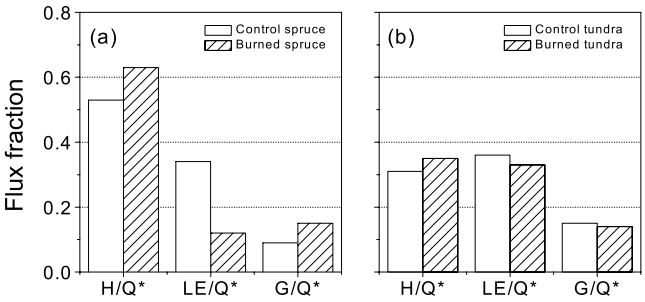

Figure 3. Relative partitioning of net radiation into turbulent and ground heat fluxes over (a) the spruce stand and (b) the tundra stand. Striped bars denote postfire values.

value compares well with the value of 0.98 often used to represent coniferous canopies [e.g., *Mahrt et al.*, 1997; *Salisbury and D'Aria*, 1992]. The corresponding 2 m air temperature (i.e., at ~75% of the mean canopy height) was 26.9 ± 0.23°C (the corresponding average 6.8 m wind speed was 1.5 m s^{-1}). On the basis of spot measurements under similar climatic conditions using a portable infrared thermometer (eight measurements conducted between 1230 and 1300 LT) the near-noon surface temperature within the burned black spruce stand (i.e., the surface seen by the atmosphere after fire removed the canopy) varied between 35 and 45°C when the air temperature at 2 m was ~25°C (the corresponding average 5.1 m wind speed was 2.1 m s^{-1}). These surface temperature estimates are consistent with radiant temperatures estimated by *Dissing et al.* [2001] from Landsat thematic mapper imagery in the summer over recent burns (46 ± 34°C) compared to nearby unburned spruce sites (26 ± 2°C). These temperature observations demonstrate a reduction of thermal coupling between the surface and atmosphere as a result of fire. From equation (2) an increase in surface temperature from 26.7 to ~40°C (i.e., 13.3°C), from the unburned to burned spruce canopy, corresponds to a decrease in net radiation of ~85 W m^{-2} (~15% reduction of net radiation based on typical midday growing season values).

[18] A similar but smaller increase in surface temperature was observed in tundra following fire. The average near-noon surface temperatures of the unburned and burned tundra sites were 11.4 and 16.5°C, respectively, when the corresponding 2 m air temperatures were 9.6 and 9.3°C. This ~5°C increase in surface temperature observed from the unburned to burned tundra corresponds to a decrease of only ~30 W m^{-2} (~7% reduction of net radiation based on typical midday growing season values).

[19] In summary, there is a net negative effect on net radiation of fire-induced changes in albedo and surface temperature for the spruce stand and a net positive effect of these changes for the tundra stand. The magnitudes of change in net radiation predicted from albedo and surface temperature estimates separately (3 − 15 = −12% and 20 − 7 = +13% for the spruce and tundra, respectively) were in close agreement with the in situ net radiation observations (−10% and +12% for the spruce and tundra, respectively). The small differences between these methods are likely attributable to the representativeness of surface temperature estimates and measurement error.

[20] The change in atmospheric coupling as a result of fire at these sites is directly related to the change in surface roughness. While fire caused a significant reduction in surface roughness over the tundra site (fourfold from z_o = 0.04 to z_o = 0.01), the change in surface roughness of the black spruce stand was considerably larger (7.8-fold from z_o = 0.70 m to z_o = 0.09 m).

[21] Independent evidence of the large fire-induced change in canopy structure of the spruce stand is provided by the change in penetration of insolation through the spruce canopy. Prior to burning, 25–35% of the daily total incoming shortwave radiation reached the understory vegetation in the unburned spruce forest, with additional radiation absorbed by understory shrubs, similar to patterns observed under a coniferous (*Pinus banksiana*) canopy [*Baldocchi et al.*, 1997]. The severe wildfire that occurred at our study site consumed all of the needles and smaller branches, leaving a relatively smooth, charred surface. After fire, more than 90% of the incident radiation above the canopy reached the blackened surface, an increase similar to that noted by *Kasischke et al.* [1995].

3.2. Surface Energy Budget

[22] Over the unburned black spruce stand the net radiation was partitioned as follows: 53% sensible heat flux, 34% latent heat flux, and 9% ground heat flux (Figure 3a). Partitioning over the burned black spruce stand was as follows: 63% sensible heat flux, 12% latent heat flux, and 15% ground heat flux. By contrast, over the unburned tundra site, the net radiation was partitioned as follows: 31% sensible heat flux, 36% latent heat flux, and 15% ground heat flux (Figure 3b). Partitioning over the burned tundra site was as follows: 35% sensible heat flux, 33% latent heat flux, and 14% ground heat flux. Regardless of stand type the effect of fire was to increase the proportion of net radiation partitioned into sensible heat flux.

[23] Note that the budget closure error ($\Delta = 1 - (H + LE + G)/Q^*$) for the burned spruce measurements (Δ_b = 0.10) was larger than for the unburned spruce measurements (Δ_{ub} = 0.04). The small-scale heterogeneity of the burned surface made it difficult to obtain a representative ground heat flux measurement. For example, there were changes in microtopography, thickness of the charred organic mat, and albedo, which was as low as 0.04 over the charred organic material that was free of loess and mineral soil. Considering the lack of canopy in the burned site (i.e., small storage term), it is likely that much of the discrepancy in closure error between the sites is due to an underestimation of the ground heat flux at the burn site.

[24] Can these results be related to spatial gradients in turbulent fluxes across a fire scar boundary that might trigger or drive a mesoscale circulation within the atmospheric boundary layer? We focus on the sensible heat flux for the purpose of this discussion. Since the burned/unburned observations for each stand type were not at adjacent sites, or were not made simultaneously, it is necessary to normalize the values of sensible heat flux before making a comparison. We normalize stand sensible heat flux fluxes with incoming shortwave radiation ($H/K_{\downarrow}$) because incident radiation is the primary energy source for turbulent exchange and is independent of surface characteristics. It would not be appropriate to normalize the sensible

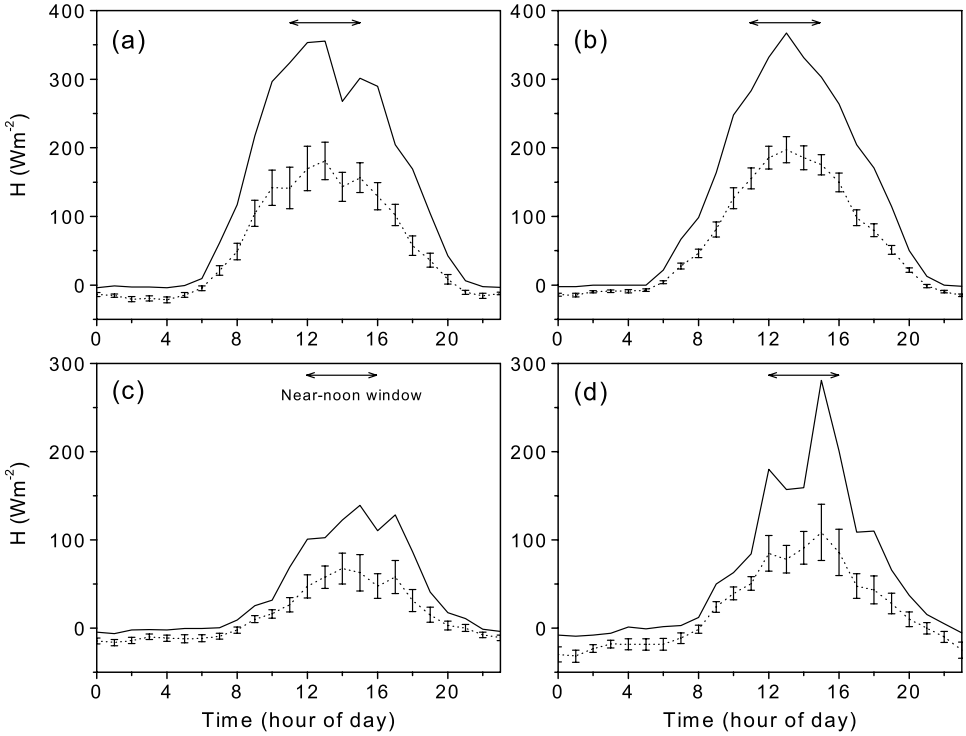

Figure 4. Diurnal composite plots of sensible heat flux over the respective measurement periods for the (a) spruce control, (b) burned spruce, (c) tundra control, and (d) burned tundra sites. Dotted lines represent mean values (with standard error), and solid lines represent the 90th percentile.

heat flux with net radiation, which is a function of surface characteristics that change after fire.

[25] In the black spruce stand, fire resulted in only a small change in normalized sensible heat flux, which increased from 0.40 to 0.43 (Table 1). On the basis of the typical clear-sky, midday value of incoming shortwave radiation for the spruce stands (754 W m^{-2}) this represents an increase in sensible heat flux of less than 20 W m^{-2}. Compared to the corresponding budget closure error of at least 50 W m^{-2} over the burned spruce stand (0.1Q*), which presumably is largely attributable to combined measurement errors given the extended fetch and simple canopy, this increase in sensible heat flux is small. For the tundra sites, normalized sensible heat flux increased from 0.20 to 0.27. On the basis of the typical clear-sky, midday value of incoming shortwave radiation for the tundra sites (615 W m^{-2}), fire caused an increase in sensible heat flux of 43 W m^{-2}, approximately equivalent to 0.1Q* for the burned tundra site.

[26] Diurnal composite mean and 90th percentile sensible heat fluxes for all four sites are presented in Figure 4. When viewed in conjunction with the results from Figure 1, it is evident that while the 90th percentile values closely resemble the reported clear-sky values, normalized sensible heat flux under mean conditions (i.e., with some cloud cover and moister soil conditions) shows a slightly larger increase as a result of fire over the spruce forest (from 0.37 to 0.41) but a slightly smaller increase over the tundra (from 0.22 to 0.26).

[27] In summary, at noon under clear-sky conditions we would not expect a significant gradient in sensible heat flux across the fire scar boundary of the black spruce stand that we observed. However, under similar conditions we would expect to see a gradient of ~50 W m^{-2} across the tundra fire scar boundary. A sensible heat flux gradient of this magnitude may be sufficient to trigger, or drive, a mesoscale circulation, depending on the size of the burn and strength of the synoptic wind field [*Shuttleworth*, 1988; *Vidale et al.*, 1997].

4. Discussion

4.1. Albedo and Net Radiation

[28] The most striking result of our study is the dramatic effects of canopy simplification on the postfire energy budget. In the tundra, where fire had only small effects on canopy architecture, surface temperature, or longwave emission, the effects of surface charring (a large reduction in albedo) dominated over effects of canopy coupling with the atmosphere, causing an increase in net radiation. In the spruce forest, however, where stem density declined threefold after fire, the smoother surface (7.8-fold reduction in roughness length) greatly reduced coupling with the atmosphere, causing an 8–18°C increase in surface temperature, a large increase in longwave emission and therefore a decrease in net radiation, despite the reduction in albedo.

[29] This large effect of canopy properties on energy budget explains both the similarities and the differences between our results and those obtained previously in Canada. In Canadian black spruce forests studied during the Boreal Ecosystem-Atmosphere Study project the canopy was more than twice as tall (10–14 m) as in the Alaskan forests (90th percentile height of 4.9 m). Consequently, the Canadian forests had somewhat different radiation efficiency and albedo ($Q^*/K_\downarrow$ = 0.79–0.84; α =

0.081–0.083) [*Kaminsky and Dubayah*, 1997; *Jarvis et al.*, 1997; *Betts and Ball*, 1997] from the forest in our study ($Q^*/K_\downarrow = 0.76$; $\alpha = 0.09$). The higher postfire albedo of the Alaskan spruce forest than of those in Canada [*Rouse*, 1976] can be attributed to the 20% cover of loess and mineral soil exposed by fire in Alaska.

[30] The unburned tundra that we studied had somewhat higher albedo than that of structurally similar tundra stands in northern Alaska [*Chapin et al.*, 2000b; *Vaganov et al.*, 2000] because of its high lichen cover. The radiation efficiency that we observed was slightly higher than values calculated from other studies [*McFadden et al.*, 1998; *Vaganov et al.*, 2000], most likely affected by the low surface temperatures. Throughout the measurement period for this site the surface was close to saturation, which would promote conductive cooling by the permafrost as well as evaporative cooling.

[31] As far as we are aware, there are no previous energy exchange measurements made over burned tundra with which to compare our data. However, general observations of many tundra burns [*Wein and Bliss*, 1973; *Wein*, 1976] suggest that the observed fire effects are typical, in that the surface is uniformly blackened by the fire, strongly reducing albedo. Tussocks ~20 cm tall govern the microtopography and "canopy" of the site and are not consumed by the fire, so changes in roughness length are expected to be minimal, as we observed.

[32] Experimental studies also suggest that canopy architecture strongly influences fire effects on energy balances. When a tall (14 m) black spruce forest was felled prior to burning, causing an extreme change in canopy density, net radiation declined after fire in spite of a large reduction in stand albedo (from 0.19 to 0.052) [*Rouse*, 1976], similar to the pattern that we observed.

[33] The differences in fire effects on net radiation between aircraft surveys by *Amiro et al.* [1999], where no significant fire effect on net radiation of spruce stands was observed, are also consistent with an important role of canopy complexity. The aircraft surveys were spatially averaged over multiple whole burn scars of heterogeneous severity, and the average height of burned tree boles was 4–5 times greater than those in our study. Consequently, the simplification of canopy architecture and reduction of surface-atmosphere coupling due to fire may have been less dramatic than for our study. In support of this the airborne surveys conducted by *Amiro et al.* [1999] indicated sensible heat fluxes 10–20% larger over recently burned coniferous forest than adjacent unburned stands, larger than the change in sensible heat flux that we observed after fire.

[34] Observations in a 1 year old burned jack pine/black spruce canopy [*Amiro*, 2001] reported a slightly reduced net radiation compared to the control stand, as well as reduced sensible heat fluxes, similar to the patterns we observed. However, these observations were made at 3 m when the standing dead tree boles averaged 13 m tall, which was noted as a potential source of error in both the net radiation and sensible heat flux observations. Net radiation measurements for our study were made both above the burned canopy and at 20% of the mean canopy height (h). On the basis of totals for the 3-week measurement period the net radiation at $0.20h$ was 12.5% lower than that measured above the canopy.

4.2. Surface Temperature

[35] The surface temperature increase observed in both biomes after fire is the combined effect of a reduction of albedo and simplification of the canopy architecture. Reducing the albedo increases the amount of net shortwave radiation that can contribute to surface heating. Extreme simplification of the canopy architecture, as in the case of burned Alaskan spruce stands, reduces the surface area over which net shortwave radiation is distributed as well as the surface area over which excess canopy heat can be shed conductively to the atmosphere. The larger increase in mean surface temperature after fire over the spruce stand reflects the substantial simplification of canopy architecture, although higher soil moisture levels in the tundra would also be a contributing factor.

[36] The tundra canopy was short and had a relatively low surface roughness both prefire and postfire. Consequently, fire did not cause a significant increase in radiation loading at the surface. Despite the simple canopy architecture a tundra surface rarely departs substantially from the 2 m air temperature because of its high albedo and high surface moisture content. Although the reduced albedo of the burned tundra surface contributes to increased surface temperatures, thermal buffering by the underlying permafrost prevents excessive excursions. The thermal conductivity of the organic material remaining after fire is greater than that of unburned tundra (because of the consumption of the lower density surface material), and permafrost retreat maintains high soil moisture levels. Consequently, there is a smaller increase in the surface-to-sky temperature difference than for black spruce, and as a result the increase in net longwave radiation associated with the increase in surface temperature due to fire in tundra is less than that for black spruce.

4.3. Heat Fluxes

[37] Fire caused little change in normalized sensible heat flux over the spruce stand but a significant change over the tundra, even though black spruce had a larger surface temperature increase following fire than tundra. This is attributable to the greater reduction in surface-atmosphere coupling over the spruce stand than the tundra following fire. The relationship between surface temperature and sensible heat flux is closely related to surface roughness [*Zeng and Dickinson*, 1998]. Vegetation surveys indicated a large reduction in stem density of remaining trees greater than 1 m in the spruce stand following fire, as well as the loss of all leaves and most of the smaller branches. Furthermore, the mean diameter at breast height of the spruce in the stand was small (less than 6 cm). On the basis of the allometric equation derived from spruce stand in this study (DBH = $0.0224h_1 - 2.4$, $R^2 = 0.77$ (DBH is in centimeters; h_1 is tree height) the DBH of spruce in a Canadian stand 10–14 m tall would be 20–29 cm. Presumably, even if a severe fire consumed the needles and many branches of a spruce stand of medium to high stem density with a canopy height between 10 and 14 m, the surface roughness would still be relatively high. The more substantial postfire canopy for the taller spruce stand would enable a greater convective heat loss to the atmosphere. The result would be a smaller mean difference in surface temperature between the burned and unburned stands and

higher sensible heat fluxes. This agrees well with the findings of *Amiro et al.* [1999], who observed no change in net radiation and a 10–20% increase in sensible heat flux after fire.

[38] Other examples of spatial heat flux gradients that oppose respective surface temperature gradients have previously been observed. *Chambers* [1998] describes measurements conducted following an extreme change in canopy characteristics, where native eucalypt forest (α = 0.10) was cleared for agriculture (α = 0.21). Although the farmland had a high albedo, the lack of a significant canopy over the harvested fields in summer contributed to the surface temperature of the farmland being ~5°C warmer than that of the adjacent forest. In spite of this surface temperature gradient, sensible heat fluxes over the farmland were ~25% lower than over the forest. A comparison was made between convective plumes in the surface layer over the 2–8 m forest canopy and farmland (harvested crops less than 0.2 m). Plume "core" temperatures over the forest were ~4°C closer to the average surface temperature than over the smooth farmland, indicating a more efficient transfer of heat to the atmosphere. There were also a larger number of plumes per kilometer encountered over the rough forest than the smooth farmland.

[39] The difference in sensible heat flux between the burned and unburned tundra of ~50 W m^{-2} compares with the contrast in heating between spruce and tundra in the vicinity of the polar front [*Pielke and Vidale*, 1995]. Thus, depending on the size (i.e., at least 5–10 km [*Avissar and Schmidt*, 1998]) and number of tundra fire scars, a heating gradient of this magnitude would be sufficient to initiate mesoscale circulations that would facilitate the mixing of warmer temperature air up into the overlying troposphere [*Andrè et al.*, 1989; *Pielke and Vidale*, 1995]. Although significant sensible heat flux gradients between unburned and early-successional to midsuccessional postfire stands have been observed in Alaskan spruce forests [*Chambers and Chapin*, 2002], no significant heating gradient was evident immediately after fire. Within 3 years after fire, however, mean summer net radiation and sensible heat flux over the same burn site were reduced compared to a nearby control stand by 10% and 14%, respectively, as a result of vegetation regrowth [*Liu et al.*, 2005]. Further, during spring, differences between the burned and control stands 3 years after fire were even more pronounced, primarily because of greater exposed snow cover and thus substantially higher albedo within the recent burn.

[40] As fire regimes of boreal and tundra regions change, there is an increasing potential for feedback to regional climate. Assuming that current parameterizations of canopy effects on the radiation balance and surface energy budget in land surface schemes are adequate, the ability of climate models to accurately predict such influences will rely heavily on suitable representation of surface characteristics (canopy architecture and albedo) of boreal regions prefire and postfire. For smooth surfaces, under strongly unstable conditions, the profile method tends to overestimate sensible heat fluxes [*Sugita et al.*, 1995]. Roughness lengths for heat and momentum directly affect sensible heat fluxes (and thus boundary layer development) and, through changes in the wind speed profile, fluxes of moisture and other scalars [*Holtslag and Ek*, 1996]. Consequently, failure to adequately account for the larger relative reduction in surface roughness following fire in short- as opposed to tall-stature black spruce stands could have important implications for regional climate prediction.

5. Conclusions

[41] We used microclimatic and eddy covariance measurements to characterize the radiation efficiency and relative partitioning of net radiation into turbulent and ground heat fluxes over two ecosystems with markedly different surface characteristics before and immediately after fire. The net effect of fire-induced changes in albedo and surface roughness on net radiation in the spruce and tundra sites were of opposite sign. The radiation efficiency ($Q^*/K_\downarrow$) of the spruce stand decreased after fire, whereas that of the tundra increased. For tundra the increase in net radiation associated with the change in albedo after fire far outweighed the decrease in net radiation resulting from the change in surface temperature. For black spruce the converse was true.

[42] Our findings indicate that the increase in surface temperature associated with the simplification of canopy architecture after fire in medium-density, low-stature black spruce forest can have a larger influence on the radiation balance than does the change in albedo. The reduction of aboveground biomass as a result of fire greatly reduces the depth and roughness of interface over which incident radiation is distributed, as well as the efficiency with which that surface can conduct heat to the atmosphere via diffusion and convection. Consequently, the surface becomes excessively hot, and radiative heat loss increases, which, in turn, reduces net radiation.

[43] Although fire resulted in a greater partitioning of net radiation into sensible heat flux over both surfaces, the contrasting responses of net radiation to fire meant that the only significant increase in sensible heat flux was over the tundra. Our observations contrast with those of *Amiro et al.* [1999], which were made over a taller spruce forest. Amiro et al. reported no significant change in net radiation following fire and an increase in sensible heat flux of 10–20 W m^{-2}. Changes in fire intensity caused by climate warming or fire management could influence the extent to which fire simplifies the canopy and reduces postfire canopy coupling. The data and mechanisms we describe will enable climate models to more accurately represent feedbacks associated with changing fire regimes.

[44] **Acknowledgments.** We thank Michelle Durant, Jay Raymond, Kevin Davey, Catharine Copass-Thompson, and Ian McHugh for their assistance in field measurements. This research was supported by grants from the National Science Foundation and U.S. Forest Service to the University of Alaska for support of the FROSTFIRE project (DEB-9707461), the Bonanza Creek Long-Term Ecological Research (LTER) program (DEB-9810217 and PNW 96-5024-2-CA), and the ATLAS project (OPP-973212).

References

Amiro, B. D. (2001), Paired-tower measurements of carbon and energy fluxes following disturbance in the boreal forest, *Global Change Biol.*, *7*, 253–268.

Amiro, B. D., J. I. MacPherson, and R. L. Desjardins (1999), BOREAS flight measurements of forest-fire effects on carbon dioxide and energy fluxes, *Agric. For. Meteorol.*, *96*, 199–208.

Amiro, B. D., J. I. MacPherson, R. L. Desjardins, J. M. Chen, and J. Liu (2003), Post-fire carbon dioxide fluxes in the western Canadian boreal

forest: Evidence from towers, aircraft and remote sensing, *Agric. For. Meteorol.*, *115*, 91–107.
Andrè, J.-C., P. Bougeault, J.-F. Mahfouf, P. Mascart, J. Noilhan, and J.-P. Pinty (1989), Impact of forests on mesoscale meteorology, *Philos. Trans. R. Soc. London, Ser. B*, *324*, 407–422.
Avissar, R., and T. Schmidt (1998), An evaluation of the scale at which ground-surface heat flux patchiness affects the convective boundary layer using large-eddy simulations, *J. Atmos. Sci.*, *55*, 2666–2689.
Baldocchi, D. D., B. B. Hicks, and T. P. Meyers (1988), Measuring biosphere-atmosphere exchanges of biologically related gases with micrometeorological methods, *Ecology*, *69*, 1331–1340.
Baldocchi, D. D., C. A. Vogel, and B. Hall (1997), Seasonal variation of energy and water vapor exchange rates above and below a boreal jack pine forest canopy, *J. Geophys. Res.*, *102*(D24), 28,939–28,951.
Baldocchi, D., F. M. Kelliher, T. A. Black, and P. Jarvis (2000), Climate and vegetation controls on boreal zone energy exchange, *Global Change Biol.*, *6*, 69–83.
Betts, A. K., and J. H. Ball (1997), Albedo over the boreal forest, *J. Geophys. Res.*, *102*(D24), 28,901–28,909.
Bonan, G. B., D. Pollard, and S. L. Thompson (1992), Effects of boreal forest vegetation on global climate, *Nature*, *359*, 716–718.
Chambers, S. D. (1998), Short- and long-term effects of clearing native vegetation for agricultural purposes, Ph.D. thesis, 178 pp., Sch. of Earth Sci., Flinders Univ., Bedford Park, Aust.
Chambers, S. D., and F. S. Chapin III (2002), Fire effects on surface-atmosphere energy exchange in Alaskan black spruce ecosystems: Implications for feedbacks to regional climate, *J. Geophys. Res.*, *108*(D1), 8145, doi:10.1029/2001JD000530.
Chapin, F. S., III, et al. (2000a), Arctic and boreal ecosystems of western North America as components of the climate system, *Global Change Biol.*, *6*, 211–223.
Chapin, F. S., III, W. Eugster, J. P. McFadden, A. H. Lynch, and D. A. Walker (2000b), Summer differences among arctic ecosystems in regional climate forcing, *J. Clim.*, *13*, 2002–2010.
Dissing, D., S. Chambers, D. Verbyla, and J. Yarie (2001), A potential wildfire-feedback mechanism in the Alaskan boreal forest: Do fire scars increase lightning activity?, paper presented at Fourth Symposium on Forest and Fire Meteorology, Am. Meteorol. Soc., Reno, Nev., 15 Nov.
Holtslag, A. A. M., and M. Ek (1996), Simulation of surface fluxes and boundary layer development over the pine forest in HAPEX-MOBILHY, *J. Appl. Meteorol.*, *35*(2), 202–213.
Jarvis, P. G., and K. G. McNaughton (1986), Stomatal control of transpiration, *Adv. Ecol. Res.*, *15*, 1–49.
Jarvis, P. G., G. B. James, and J. J. Landsberg (1976), Coniferous forest, in *Vegetation and the Atmosphere*, vol. 2, edited by J. L. Monteith, pp. 171–240, Elsevier, New York.
Jarvis, P. G., J. M. Massheder, S. E. Hale, J. B. Moncrieff, M. Rayment, and S. L. Scott (1997), Seasonal variation of carbon dioxide, water vapor, and energy exchanges of a boreal black spruce forest, *J. Geophys. Res.*, *102*(D24), 28,953–28,966.
Kaminsky, K. Z., and R. Dubayah (1997), Estimation of surface net radiation in the boreal forest and northern prairie from shortwave flux measurements, *J. Geophys. Res.*, *102*(D24), 29,707–29,716.
Kasischke, E. S., N. L. Christensen Jr., and B. J. Stocks (1995), Fire, global warming, and the carbon balance of boreal forests, *Ecol. Appl.*, *5*, 437–451.
Leuning, R., and M. J. Judd (1996), The relative merits of open- and closed-path analysers for measurement of eddy fluxes, *Global Change Biol.*, *2*, 241–253.
Liu, H., J. T. Randerson, J. Lindfors, and F. S. Chapin III (2005), Changes in the surface energy budget after fire in boreal ecosystems of interior Alaska: An annual perspective, *J. Geophys. Res.*, doi:10.1029/2004JD005158, in press.
Mahrt, L., J. Sun, J. I. MacPherson, N. O. Jenses, and R. L. Desjardins (1997), Formulation of surface heat flux: Applications to BOREAS, *J. Geophys. Res.*, *102*(D24), 28,901–28,909.
McCaughey, J. H., and W. L. Saxon (1998), Energy balance storage terms in a mixed forest, *Agric. For. Meteorol.*, *44*, 1–18.
McFadden, J. P., F. S. Chapin III, and D. Y. Hollinger (1998), Subgrid-scale variability in the surface energy balance of arctic tundra, *J. Geophys. Res.*, *103*(D22), 28,947–28,961.
Meesters, A. G. C. A., and H. F. Vugts (1996), Calculation of heat storage terms, *Agric. For. Meteorol.*, *78*, 181–202.
Murphy, P. J., J. P. Mudd, B. J. Stocks, E. S. Kasischke, D. Barry, M. E. Alexander, and N. H. F. French (2000), Historical fire records in the North American boreal forest, in *Fire, Climate Change and Carbon Cycling in Boreal Forest*, edited by E. S. Kasischke and B. J. Stocks, pp. 275–288, Springer, New York.
Oke, T. R. (1987), *Boundary Layer Climates*, 435 pp., Methuen, New York.
Pielke, R. A., and P. L. Vidale (1995), The boreal forest and the polar front, *J. Geophys. Res.*, *100*(D12), 25,755–25,758.
Radiation and Energy Balance Systems (1994), REBS *Q**7 net radiometer manual, revision 1, Seattle, Wash.
Röser, C., L. Montagnani, E.-D. Schulze, D. Mollicone, O. Kolle, M. Meroni, D. Papale, L. B. Marchesini, S. Federici, and R. Valentini (2002), Net CO_2 exchange rates in three different successional stages of the "dark taiga" of central Siberia, *Tellus, Ser. B*, *54*, 642–654.
Rouse, W. R. (1976), Microclimatic changes accompanying burning in subarctic lichen woodland, *Arct. Alp. Res.*, *8*, 357–376.
Salisbury, J., and D. D'Aria (1992), Emissivity of terrestrial materials in the 8–14 μm atmospheric window, *Remote Sens. Environ.*, *42*, 83–106.
Schmid, H. P. (1997), Experimental design for flux measurements: Matching scales of observations and fluxes, *Agric. For. Meteorol.*, *87*, 179–200.
Shuttleworth, W. J. (1988), Macrohydrology: The new challenge for process hydrology, *J. Hydrol.*, *100*, 31–56.
Stenberg, P., E. H. DeLucia, A. W. Schoette, and H. Smolander (1995), Photosynthetic light capture and processing from cell to canopy, in *Resource Physiology of Conifers*, edited by W. K. Smith and T. M. Hinckley, pp. 3–38, Elsevier, New York.
Sugita, M., T. Hiyama, N. Endo, and S.-F. Tian (1995), Flux determination over a smooth surface under strongly unstable conditions, *Boundary Layer Meteorol.*, *73*, 145–158.
Thomas, G., and P. R. Rowntree (1992), The boreal forests and climate, *Q. J. R. Meteorol. Soc.*, *118*, 469–497.
Vaganov, E., et al. (2000), Land-atmosphere energy exchange in arctic tundra and boreal forest: Available data and feedbacks to climate, *Global Change Biol.*, *6*, 84–115.
Vidale, P. L., R. A. Pielke, L. T. Steyaert, and A. Barr (1997), Case study modeling of turbulent and mesoscale fluxes over the BOREAS region, *J. Geophys. Res.*, *102*(D24), 29,167–29,188.
Wein, R. W. (1976), Frequency and characteristics of arctic tundra fires, *Arctic*, *29*, 213–222.
Wein, R. W., and L. C. Bliss (1973), Changes in arctic *Eriophorum* tussock communities following fire, *Ecology*, *54*, 845–852.
Whittaker, R. H. (1975), *Communities and Ecosystems*, 2nd ed., Macmillan, New York.
Zeng, X., and R. E. Dickinson (1998), Effect of surface sublayer on surface skin temperature and fluxes, *J. Clim.*, *11*, 537–550.

J. Beringer, School of Geography and Environmental Science, Monash University, Wellington Road, Clayton, Vic 3168, Australia.
S. D. Chambers, ANSTO Environment, Australian Nuclear Science and Technology Organization, PMB 1, Menai, NSW 2234, Australia. (szc@ansto.gov.au)
F. S. Chapin III, Institute of Arctic Biology, University of Alaska Fairbanks, Fairbanks, AK 99775-7000, USA.
J. T. Randerson, Department of Earth System Science, University of California, Irvine, CA 92697, USA.